Optical-absorption spectra of $CsFeCl_3 \cdot 2H_2O$. I. Temperature dependence

H. Okada, N. Kojima, T. Ban, and I. Tsujikawa
Department of Chemistry, Kyoto University, Kyoto 606, Japan
(Received 9 January 1990; revised manuscript received 23 August 1990)

The quasi-one-dimensional Ising-like antiferromagnet $CsFeCl_3 \cdot 2H_2O$ has been studied by experiments on the absorption spectra corresponding to the ${}^5T_2(D) \rightarrow \{{}^3T_2(G), {}^3T_1(F), {}^3A_2(F)\}$ transition of the Fe^{2+} ion in the 1.5–77-K region. These spectra consist of exciton lines and their satellite absorption lines,and some of the absorption lines are concluded to be associated with thermally excited magnetic domain walls. The temperature variation of these spectra shows the following: above about T_N (12.75 K), domain-wall excitation plays an important role in the magnetically disordering process with the rise of temperature; additionally, above about 30 K, excitation to the second lowest excited state also contributes to this process. The temperature dependence of the intensities of the spectra is explained by Boltzmann statistics, taking account of these excitations.

I. INTRODUCTION

$CsFeCl_3 \cdot 2H_2O$ (CFC) has bee studied by various experiments[1–8] and is shown to be a quasi-one-dimensional Ising-like antiferromagnet. Its crystal structure determined by neutron-diffraction experiments is sketched in Fig. 1. The structure consists of *cis*-$[FeCl_4(H_2O)_2]^2$ octahedra, which are strongly coupled along the a axis by a shared Cl^- ion. The resulting chains are weakly coupled along the b axis by Cs^+ ions and along the c axis by hydrogen bonds. Thus, the superexchange interaction between the neighboring Fe^{2+} ions along the a axis (intrachain) is much stronger than those along the b and c axes (interchain). Its magnetic behavior at low temperatures can be described by effective spin $S=\frac{1}{2}$, because the pseudodoublet ground state lies more than 40 K below the first excited state.[2,9] On the basis of the Ising model, the intrachain and the interchain interactions have been estimated to be $J_a/k=-40.4$ K and $(J_b+J_c)/k=-0.7$ K, respectively, from magnetization experiments.[1,8] The small interchain interactions induce three-dimensional magnetic order below $T_N=12.75$ K.[6] Its magnetic structure determined by neutron-diffraction and nuclear magnetic resonance (NMR) experiments[1] is sketched in Fig. 2. The magnetic moments are located in the ac plane at an angle of 15° from the a axis. Its spin-relaxation mechanism has been studied by Mössbauer and NMR experiments,[3,4] and the existence of thermally excited magnetic domain walls has been suggested.

Generally, magnetic domain walls in one-dimensional Ising-like antiferromagnets have the following feature. The domain-wall, e.g., $\cdots\downarrow\uparrow\downarrow\uparrow\uparrow\downarrow\uparrow\cdots$, can be excited with the rise of temperature and is localized between two adjacent spins within a chain. In Ising-like systems, which are described by

$$\mathcal{H}=2J\sum_i [S_i^z S_{i+1}^z+\epsilon(S_i^x S_{i+1}^x+S_i^y S_{i+1}^y)]$$

and

$$0<|\epsilon|\ll 1\ ,$$

the domain wall can move along the chain owing to the small transverse exchange interaction and behaves like an elementary excitation.[10] This domain-wall excitation can be classified into two kinds, namely, single domain-wall and domain-wall pair excitation. The single domain-wall excitation takes place at a chain end, and one domain wall created by this excitation is able to move along the chain. This process is described, for example, as follows:

$$\cdots\downarrow\uparrow\downarrow\uparrow\downarrow\uparrow\rightarrow\cdots\downarrow\uparrow\downarrow\uparrow\uparrow\downarrow\rightarrow\cdots\downarrow\uparrow\uparrow\downarrow\uparrow\downarrow\ .$$

The thermal activation energy of the single domain-wall excitation is approximately $|J|$. On the other hand, the domain-wall pair excitation takes place within a chain and creates two domain walls. Then, magnon excitation (one-spin-cluster excitation), e.g.,

$$\cdots\downarrow\uparrow\downarrow\uparrow\downarrow\uparrow\downarrow\cdots\rightarrow\cdots\downarrow\uparrow\downarrow\downarrow\downarrow\uparrow\downarrow\cdots$$

and several-spins-cluster excitation, e.g.,

$$\cdots\downarrow\uparrow\downarrow\uparrow\downarrow\uparrow\downarrow\cdots\rightarrow\cdots\downarrow\uparrow\uparrow\downarrow\uparrow\uparrow\downarrow\cdots$$

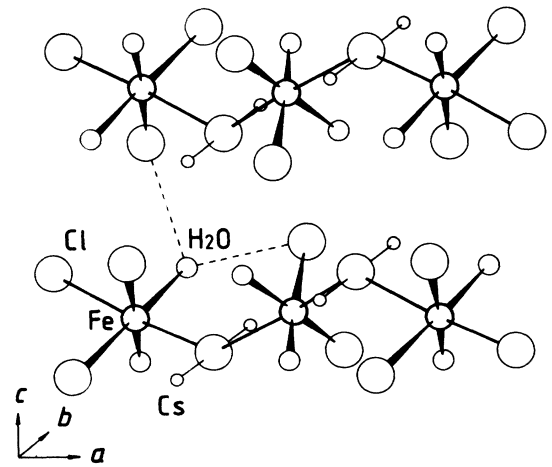

FIG. 1. Crystal structure of $CsFeCl_3 \cdot 2H_2O$. The dashed lines show one set of hydrogen bonds.

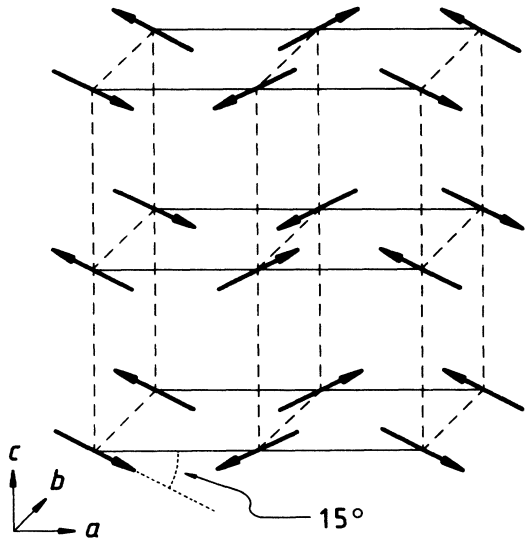

FIG. 2. Magnetic structure of $CsFeCl_3 \cdot 2H_2O$. Spins are located in the *ac* plane at an angle of 15° from the *a* axis.

can be taken as the domain-wall pair excitation.[11] The magnon excitation (one-spin-cluster excitation) corresponds to the domain-wall pair excitation reversing a single spin, and the several-spins-cluster excitation corresponds to that reversing more than two spins. Of course, the domain walls created by the domain-wall pair excitation are able to move along the chain. Consequently, the number of spins between the domain-wall pair can change with time. The thermal activation energy of the domain-wall pair excitation is approximately $2|J|$. Such a domain-wall excitation having the above feature is expected to govern thermal magnetic excitation in one-dimensional Ising-like antiferromagnets.[12]

Now we have studied the magneto-optical property of CFC by experiment on its absorption spectra under various conditions. In the present paper and in paper II,[13] we report the result of this study by examining the dependence of the spectra on temperature and magnetic fields, respectively. The main purpose of the present paper is to investigate the influence of the domain walls on the spectra and to reveal the behavior of the domain walls. Moreover, the present paper deals with other thermal excitations.

II. EXPERIMENTAL PROCEDURE

The crystals of CFC were grown at room temperature by slow evaporation from an aqueous solution of $FeCl_2 \cdot 4H_2O$ and CsCl in a molar ratio of 1:2. To prevent oxidation of Fe^{2+} ions, HCl was added to this solution as far as pH=2, and this solution was kept in a N_2 atmosphere. In this way, the large single crystals were obtained with typical dimensions of $20 \times 15 \times 5$ mm^3. These crystals look pale brown and may be easily cleaved parallel to the largest crystal face corresponding to the *ab* plane.

The absorption spectra below 77 K were measured with a tungsten-iodine projection lamp, a Jobin-Yvon model THR-1500 grating spectrometer, and a Hamamatsu photonics model R-376 photomultiplier. The accuracy of this measurement was ±0.004 nm for sharp absorption lines. The absorption spectra at 300 K were measured with a Cary 17D grating spectrometer.

In the measurement at 77 and 1.5 K, the sample was immersed in liquid nitrogen and pumped liquid helium, respectively. In the measurement from 2 to 70 K, the sample was fastened to a holder by Apiezon N grease and was placed with exchange helium gas into a glass vessel immersed in pumped liquid helium. The sample holder was made of copper and was equipped with a carbon glass thermometer and an electric heater. By the adjustment of the electric power of this heater, the temperatures of the sample could be controlled to about ±1%.

A uniaxial stress was generated by the apparatus consisting of an oil-press pump, a stainless-steel piston cylinder, and a sample holder.

III. ASSIGNMENT OF THE ABSORPTION SPECTRA

A. Crystal-field spectrum

The absorption spectrum of CFC at 300 K in the 5000–33 000-cm^{-1} region is shown in Fig. 3. With crystal-field theory, we interpret this spectrum as follows. The strong, splitting band below 12 000 cm^{-1} is assigned to the spin-allowed transition $^5T_2(D) \rightarrow {}^5E(D)$, and its splitting is occasioned by the spin-orbit interaction and the low-symmetry crystal field. The weak bands above 12 000 cm^{-1} are assigned to the spin-forbidden transitions. Each assignment of them is shown in Fig. 3, but the decided assignments cannot have been obtained in the 18 000–28 000-cm^{-1} region, because many weak bands overlap with one another in this region.

B. Effect of uniaxial stress

The absorption spectra of CFC have considerable fine structures at sufficiently low temperatures in the

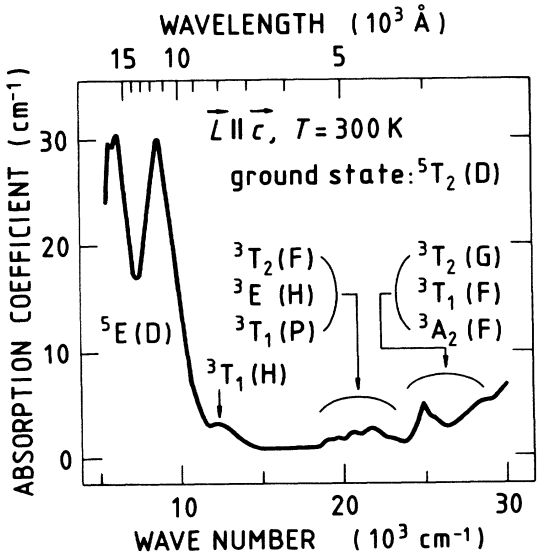

FIG. 3. Absorption spectrum of $CsFeCl_3 \cdot 2H_2O$ at 300 K. The incident light was parallel to the *c* axis.

24 150–24 900-cm^{-1} region, where all the absorption lines have electric-dipole character. The lowest-energy part of these structures at 1.5 K is shown in Fig. 4. The labeling of the absorption lines is based on the following uniaxial stress experiment.

As shown in Fig. 5, the six absorption lines can be classified into two groups by the difference in their energy shifts with the stress parallel to the c axis; three of them have the small shift, 5.5×10^{-2} $cm^{-1}MPa^{-1}$, and the others have the large shift, 1.2×10^{-1} $cm^{-1}MPa^{-1}$. Then, the former absorption lines are labeled $A0$, $A1$, and $A2$, respectively (A group), and the latter absorption lines are labeled $B0$, $B1$, and $B2$, respectively (B group).[14]

The stress applied to the sample is able to change the energies of elementary excitations, namely, excitons, phonons, magnons, and domain walls. However, by reference to the reports of several other magnetic compounds,[15–17] we assume that this stress changes only the exciton energies. This assumption draws the following conclusion from the above experimental result. Two distinct excitations contribute to the absorption lines shown in Fig. 4; one contributes to the A group and the other contributes to the B group.

Figures 6 and 7 show the temperature variation of the fine structure in the a polarization (**E**||**a**). The $A1$ line cannot be observed above about 20 K owing to an extra absorption line. The absorption lines observed only at higher temperatures are labeled as $H1$, $H2$, $H3$, and $H4$, respectively.

The uniaxial stress experiment at 77 K proves that the $H3$ line belongs to the A group; but the stress effect on $H1$, $H2$, and $H4$ cannot have been examined, for they are weak and broad. Nevertheless, we suppose that the

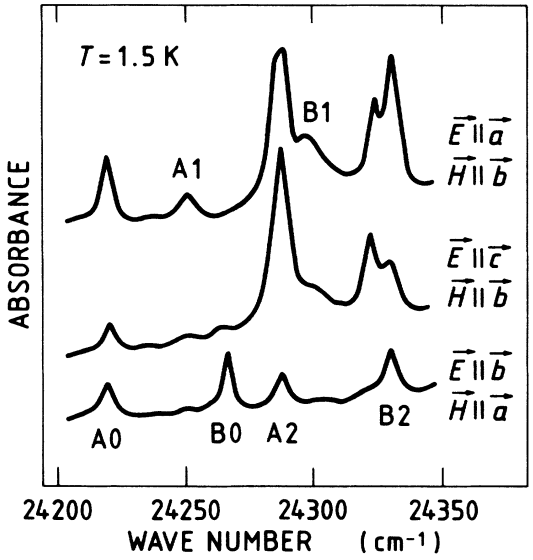

FIG. 4. Polarized absorption spectra in the lowest energy region of the ${}^5T_2(D)\rightarrow\{{}^3T_2(G),{}^3T_1(F),{}^3A_2(F)\}$ transition of $CsFeCl_3\cdot2H_2O$ at 1.5 K. The symbols **E** and **H** denote the electric and magnetic vectors of the incident light, respectively. As regards the absorption line observed between $B1$ and $B2$, see Ref. 14.

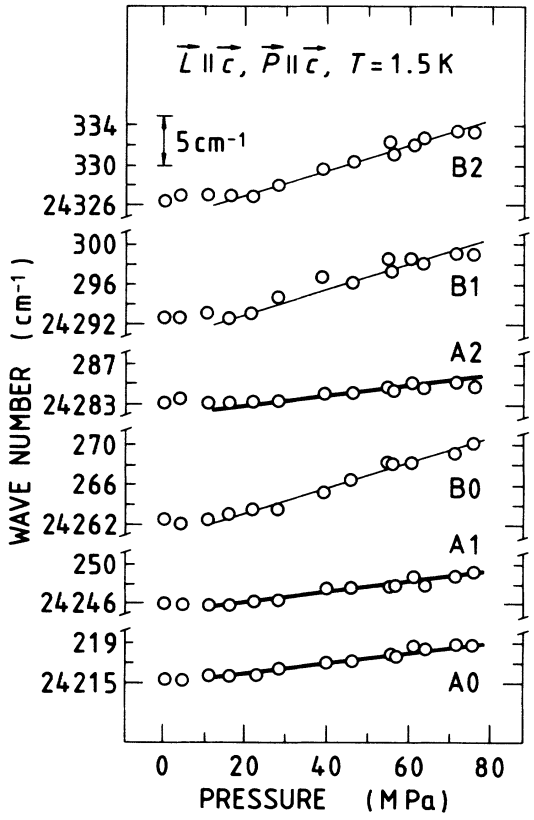

FIG. 5. Energy shifts of the $A0$, $A1$, $A2$, $B0$, $B1$, and $B2$ lines at 1.5 K with the stress parallel to the c axis. The incident light is parallel to the c axis. The slopes of the thick and the thin solid lines are 5.5×10^{-2} and 1.2×10^{-1} cm^{-1} MPa^{-1}, respectively.

$H1$, $H2$, and $H4$ lines belong to the A group. This supposition is probably true, because four other absorption lines regarded as the corresponding $H1$, $H2$, $H3$, and $H4$ lines of the B group have been observed in **E**||**b**.

In what follows, only the A group is discussed. The peak energies of the absorption lines are summarized in Table I.

C. $A0$, $A1$, and $A2$ lines

From Fig. 4, it can be seen that the $A0$ line has the lowest peak energy and the narrowest half-width in the A

TABLE I. Peak energies of absorption lines and temperature regions where each of the absorption lines is observed.

Label	Peak energy (cm^{-1})	Temperature region (K)
$A0$	24 217.1 (1.5 K)	$\lesssim 50$
$A1$	24 246.6 (1.5 K)	$\lesssim 18$
$A2$	24 284.2 (1.5 K)	all regions
$H1$	24 249.1 (12.7 K)	12–50
$H2$	24 201.1 (28.3 K)	27–36
$H3$	24 186.4 (12.7 K)	$10\lesssim$
$H4$	24 134.2 (50.0 K)	$50\lesssim$

group at 1.5 K. Additionally, as shown in Fig. 8, integrated intensity of the $A0$ line is almost constant below T_N and decreases with the rise of temperature above T_N. From these results, we conclude that the $A0$ line is an exciton line. The decrease in its intensity is caused by the increase in the thermal population of excited states. The detailed analysis of this decrease (the solid curve in Fig. 8) is discussed in the next section.

The $A1$ and $A2$ lines have peak energies that are higher than those of the $A0$ line by 29.5 and 67.1 cm^{-1}, respectively, at 1.5 K, and their intensities do not increase with temperature. Their transition mechanisms are determined in paper II,[13] and the present paper does not deal any further with them.

D. $H1$ and $H3$ lines

As shown in Figs. 6 and 7, there $H3$ line is observed above 10 K, and its peak energy is lower than that of the $A0$ line by about 29 cm^{-1}, being almost constant up to

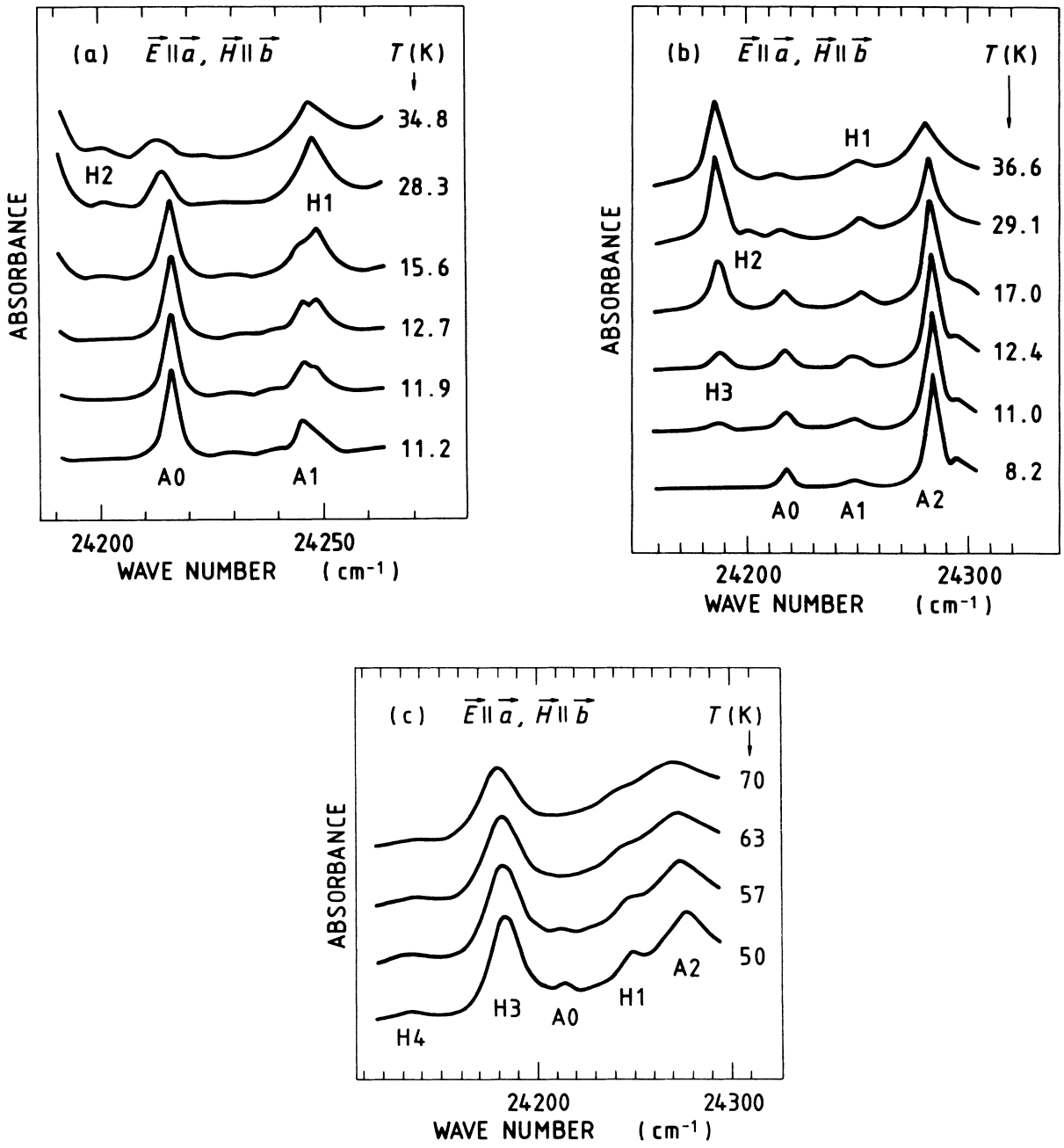

FIG. 6. Absorption spectra in the lowest energy region of the ${}^5T_2(D) \rightarrow \{{}^3T_2(G), {}^3T_1(F), {}^3A_2(F)\}$ transition of $CsFeCl_3 \cdot 2H_2O$ in E||a at various temperatures: (a) from 11.2 to 34.8 K in the 24 190–24 260-cm^{-1} region; (b) from 8.2 to 36.6 K in the 24 160–24 300-cm^{-1} region; (c) from 50 to 70 K in the 24 100–24 300-cm^{-1} region.

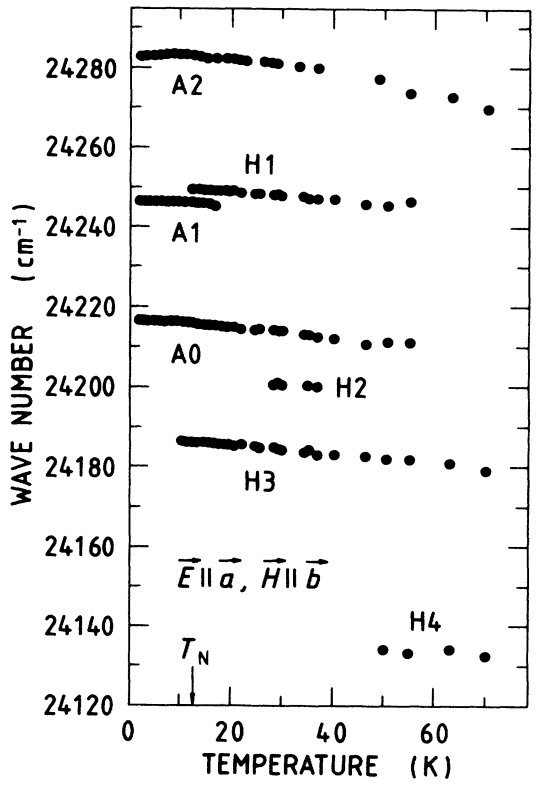

FIG. 7. Energy shifts of the $A0$, $A1$, $A2$, $H1$, $H2$, $H3$, and $H4$ lines with the rise of temperature.

50 K. This energy difference is closely equal to the intrachain interaction ($J_a = -28$ cm^{-1}). The temperature variation of the integrand intensity of the $H3$ line is shown in Figs. 9(a) and 9(b). The solid line in Fig. 9(b) is computed using a least-squares program in the 12.7 K (about T_N) to 21.7 K region and indicates that the integrated intensity varies with temperature agreeably to exp($-|J_a|/kT$) in this region. Taking account of these experimental data, we attribute the $H3$ line to the $A0$ exciton creation at a thermally excited magnetic domain-wall site, e.g., $\cdots\downarrow\uparrow\downarrow\bar{\uparrow}\uparrow\downarrow\uparrow\cdots$ (the overbar expresses the site under discussion). In other words, the $H3$ line is assigned to the electronic transition from the

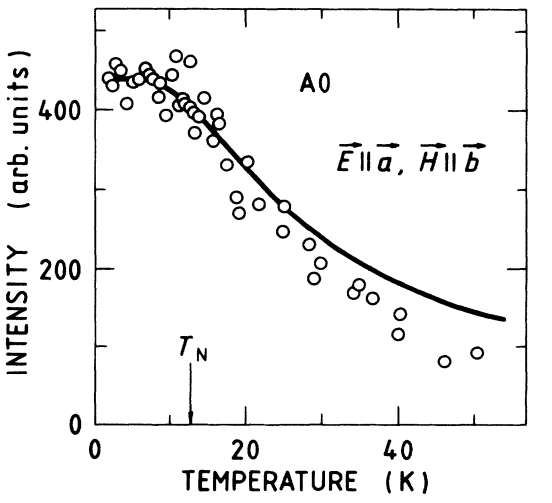

FIG. 8. Temperature variation of the integrated intensity of the $A0$ line. The solid curve is discussed in the text.

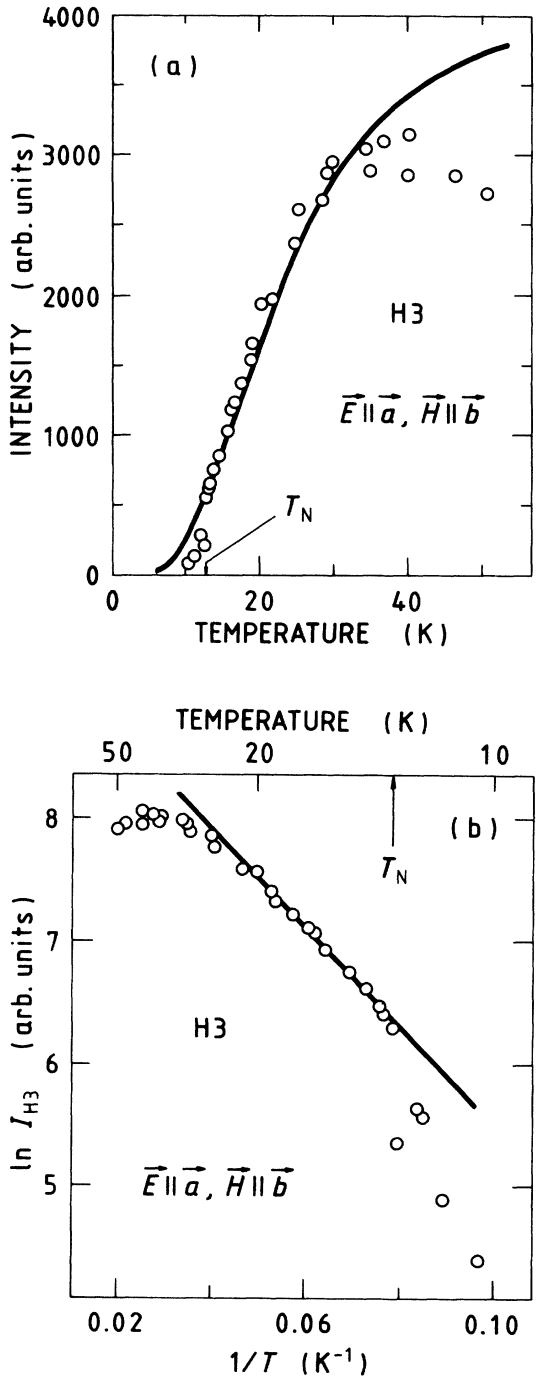

FIG. 9. Temperature variation of the integrated intensity of the $H3$ line: (a) on a linear scale; (b) on a logarithmic scale. The solid curve in (a) is discussed in the text. The solid line in (b) is computed using a least-squares program in the 12.7–21.7-K region, and its slope is -40.0 K, which is almost equal to the intrachain interaction ($J_a/k = -40.4$ K).

ground state of such a domain-wall site to the corresponding excited state of the $A0$ line (see Fig. 10). Such an absorption line attributed to an exciton creation at a domain-wall site has been observed in $CsCoCl_3$.[18]

The $H3$ line is considered to be associated almost only with single domain-wall excitation in the 12.7–21.7-K region, because its intensity varies in accordance with $\exp(-|J_a|/kT)$, not with $\exp(-|2J_a|/kT)$, in this region. However, the temperature variation of its intensity deviates from $\exp(-|J_a|/kT)$ below T_N and above 21.7 K. The deviation below T_N is due to the three-dimensional magnetic order, which suppresses the domain-wall movement. On the other hand, the deviation above 21.7 K is due to other thermal excitations, for example, domain-wall pair excitation. The analysis of the influence of other thermal excitations [the solid curve in Fig. 9(a)] is discussed in the next section.

As shown in Figs. 6 and 7, the $H1$ line is observed above about 10 K, and its peak energy is higher than that of the $A1$ line by about 3 cm^{-1}. The intensity of the $H1$ line increases with temperature, so then the $A1$ line cannot be observed above about 20 K. The transition mechanism of the $H1$ line is determined in paper II,[13] and the present paper does not deal any further with the $H1$ line.

E. Hot-magnon sideband

A hot-magnon sideband discussed here is an absorption band assigned to an exciton creation at a thermally excited magnon site, e.g., $\cdots\downarrow\uparrow\downarrow\bar{\downarrow}\downarrow\uparrow\downarrow\cdots$. Its peak energy will be lower than that of its original exciton line by the excitation energy of the magnon with $\mathbf{k}=0$, and such magnon excitation energy in an Ising-like magnet will be estimated at approximately $2|J|$. This estimation in $RbFeCl_3 \cdot 2H_2O$, which has a property similar to CFC, has been verified by far-infrared transmission experiments.[19] Consequently, we can presume that the hot-magnon sideband of the $A0$ line appears about 56 cm^{-1} below the $A0$ line. Nevertheless, such an absorption band has not been observed in this experiment, though the temperatures (up to 77 K) are high enough for the thermal excitation of the magnon. We interpret this result as follows.

As mentioned in Sec. I, a magnon in CFC is equivalent to a domain-wall pair containing a single spin, and these domain walls can move along a chain. Thus, a magnon excited state (a one-spin-cluster excited state) is expected to transform itself with time into a several-spins-cluster excited state. In other words, a magnon site does not remain as it is, and this site changes itself with time into a domain-wall site, e.g.,

$$\cdots\downarrow\uparrow\downarrow\bar{\downarrow}\downarrow\uparrow\downarrow\uparrow\downarrow\cdots\rightarrow\cdots\downarrow\uparrow\downarrow\bar{\downarrow}\uparrow\downarrow\downarrow\uparrow\downarrow\cdots .$$

Of course, the reverse change can occur, and a several-spins-cluster excited state transforms itself into a magnon excited state. However, the number of the magnon sites in this case is much smaller than that in the case when the domain-wall movement is disregarded. Therefore, the intensities of the hot-magnon sidebands in CFC will be very weak even at high temperatures, so the hot-magnon sideband of the $A0$ line has not been observed in this experiment.

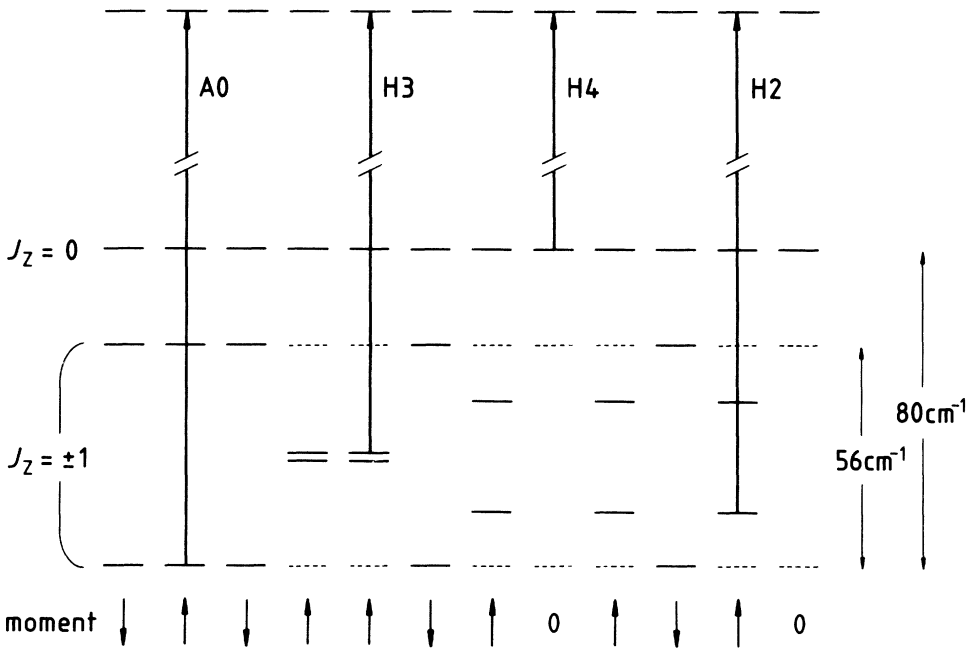

FIG. 10. Excitation schemes for the $A0$, $H3$, $H4$, and $H2$ lines. The symbols ↑, ↓, and 0 described at the bottom express the magnetic moment of each site within a chain in the initial state of these excitations, and J_z denotes the total angular momentum. The lines represent the energy levels of each site.

F. $H2$ and $H4$ lines

As shown in Figs. 6 and 7, the very weak but evident absorption lines $H2$ and $H4$ are observed on the lower-energy side of the $A0$ line in the 27–36-K region and above about 50 K, respectively. The energy differences between the $A0$ line and these absorption lines are about 13 and 78 cm^{-1}, respectively, in these temperature regions. These energy differences cannot be explained by domain-wall or magnon excitation; then, the second lowest excited state must be taken into account. Our experiment with magnetic fields[13] shows this excited state to be a singlet state and to lie about 80 cm^{-1} higher than the ground state at 1.5 K. This energy difference, 80 cm^{-1}, is nearly equal to that between the $A0$ and $H4$ lines, 78 cm^{-1}. From these experimental data, we draw the conclusion that the $H4$ line is ascribed to the electronic transition from the second lowest excited state to the corresponding excited state of the $A0$ line. That is to say, the $H4$ line is assigned to the $A0$ excitation creation at such a thermally excited singlet-state site, e.g., $\cdots\downarrow\uparrow\downarrow\bar{0}\downarrow\uparrow\downarrow\cdots$ (the symbol 0 represents the singlet state). Its transition mechanism is illustrated in Fig. 10.

Since this second lowest excited state has no magnetic moment, the internal magnetic field at an adjacent site along a chain, e.g., $\cdots\downarrow\uparrow\bar{\downarrow}0\downarrow\uparrow\downarrow\cdots$, will be half as large as that at a Néel-state site, e.g., $\cdots\downarrow\uparrow\bar{\downarrow}\uparrow\downarrow\uparrow\downarrow\cdots$. Thus, the ground state of such an adjacent site will be higher than the Néel state by $|J_a|/2=14$ cm^{-1}, which is schematically shown in Fig. 10. The value 14 cm^{-1} closely agrees with the energy difference 13 cm^{-1} between the $A0$ and $H2$ lines. Considering the above, we attribute the $H2$ line to the $A0$ excition creation at a site that is adjacent to a thermally excited singlet-state site (see Fig. 10). By the way, the $H2$ line disappears above 36 K, not because its intensity decreases but because the $H3$ line is broadened.

IV. INTENSITIES OF THE $A0$ AND $H3$ LINES

In this section, the temperature dependence of the integrated intensities of the $A0$ and $H3$ lines is quantitatively discussed. Initially, we suppose that only the nearest-neighbor intrachain interaction exerts influence on the state of each site, and so only a single chain is treated in this section. With the rise of temperature, the following thermal excitations are able to take place in the chain: single domain-wall excitation, several-spins-cluster excitation, and excitation to the second lowest excited state. Their activation energies are 40.4, 80.8, and 116 K, respectively. Magnon excitation (one-spin-cluster excitation) is not taken into account here, because, as mentioned in Sec. III E, its excited state is expected to transform itself into the several-spins-cluster excited state. Other thermal excitations are also neglected.

At this stage, the symbols used below shall be defined. The symbol N denotes the number of all sites in the chain, and N_G denotes the number of Néel-state sites in this chain. The symbols N_d, N_c, and N_s denote the numbers of the single domain-wall excitations, the several-spins-cluster excitations, and the excitations to the second lowest excited state in this chain, respectively. The integrated intensities of the $A0$ and $H3$ lines are expressed by I_{A0} and I_{H3}, respectively.

Here, we suppose the following: (i) There are no interactions between the thermal excitations; (ii) Domain walls, including ones created at a chain end, are able to move throughout the chain in the interval of about 5 min, which is the time between temperature changing and measurement beginning; (iii) Domain walls hardly move, while one exciton is created; in other words, the rate of the domain-wall motion is much slower than that of the exciton creation.

Since the excited states are localized, they are considered to satisfy Boltzmann statistics. Then, the temperature dependence of the populations of these excitations is given by

$$\begin{aligned} N_d/N_G &= \exp(-40.4/T)\ , \\ N_c/N_G &= \exp(-80.8/T)\ , \\ N_s/N_G &= \exp(-116/T)\ . \end{aligned} \tag{1}$$

It is clear that $N_G \simeq N$ at very low temperatures. As temperature rises, N_d, N_c , and N_s increase; simultaneously, N_G decreases. One single domain-wall excitation changes two Néel-state sites into two domain-wall sites, e.g.,

$$\cdots\downarrow\uparrow\downarrow\uparrow\bar{\downarrow}\bar{\uparrow}\downarrow\uparrow\rightarrow\cdots\downarrow\uparrow\downarrow\uparrow\bar{\downarrow}\bar{\downarrow}\uparrow\downarrow$$

and one several-spins-cluster excitation changes four Néel-state sites into four domain-wall sites, e.g.,

$$\cdots\downarrow\bar{\uparrow}\bar{\downarrow}\uparrow\bar{\downarrow}\bar{\uparrow}\downarrow\cdots\rightarrow\cdots\downarrow\bar{\uparrow}\bar{\uparrow}\downarrow\bar{\uparrow}\bar{\downarrow}\downarrow\cdots\ .$$

In addition, one excitation to the second lowest excited state changes three Néel-state sites into one singlet-state site and two excited-state sites associated with the $H2$ line, e.g.,

$$\cdots\downarrow\uparrow\bar{\downarrow}\bar{\uparrow}\bar{\downarrow}\uparrow\downarrow\cdots\rightarrow\cdots\downarrow\uparrow\bar{\downarrow}\bar{0}\bar{\downarrow}\uparrow\downarrow\cdots\ .$$

Accordingly, one single domain-wall excitation, one several-spins-cluster excitation, and one excitation to the second lowest excited state decrease N_G by 2, 4, and 3, respectively; the relation between them is given by

$$N_G = N - 2N_d - 4N_c - 3N_s\ . \tag{2}$$

Put Eq. (1) into this relation, then,

$$\frac{N_G}{N} = \frac{1}{1+2\exp(-40.4/T)+4\exp(-80.8/T)+3\exp(-116/T)}\ . \tag{3}$$

If the several suppositions mentioned up to this point are valid for the actual thermal excitations, the temperature dependence of I_{A0} will be described by

$$I_{A0} \propto \frac{1}{1+2\exp(-40.4/T)+4\exp(-80.8/T)+3\exp(-116/T)} . \quad (4)$$

The solid curve in Fig. 8, which is normalized at 1.5 K, represents formula (4) and finely fits in with the experimental result.

As mentioned in Sec. III D, the $H3$ line is attributed to the $A0$ exciton creation at a domain-wall site. Thus, I_{H3} will be proportional to the number of domain-wall sites. One single domain-wall excitation and one several-spins-cluster excitation create two and four domain-wall sites, respectively. In a manner similar to I_{A0}, the temperature dependence of I_{H3} will be described by

$$I_{H3} \propto \frac{2\exp(-40.4/T)+4\exp(-80.8/T)}{1+2\exp(-40.4/T)+4\exp(-80.8/T)+3\exp(-116/T)} . \quad (5)$$

The solid curve in Fig. 9(a), which is normalized at T_N, represents formula (5) and fits in well with the experimental result.

Formulas (4) and (5) explain satisfactorily the temperature dependence of I_{A0} and I_{H3}, respectively. This fact verifies the suppositions in this section. However, as can be seen from Fig. 9(a), there is the disagreement of I_{H3} between the experimental and the theoretical result at higher temperatures. The most important cause of this disagreement is probably not taking account of magnon excitation. Since the density of the domain walls is high at sufficiently high temperatures, several magnon sites will be able to exist at these temperatures even under domain wall movement. Such magnon sites will contribute to the above-mentioned disagreement. Besides, the supposition that there are no interactions between the thermal excitations comes into question at higher temperatures. Formula (5) indicates that the thermal equilibrium occupancy of domain-wall sites is, for example, 0.42 at 40 K and 0.29 at 25 K. This value, 0.29 at 25 K, is consistent with the spin-spin correlation length within a chain, about 3.7 spins at 25 K, which is measured by neutron scattering.[6] At such high temperatures, the interaction between the thermal excitations is expected to exist and to contribute to the above-mentioned disagreement.

V. CONCLUSION

The optical-absorption spectra of CFC have fine structures at sufficiently low temperatures in the 24 150–24 350-cm^{-1} region. These fine structures are attributed to the $^5T_2(D) \rightarrow \{^3T_2(G), ^3T_1(F), ^3A_2(F)\}$ transition of the Fe^{2+} ion and consist of two exciton lines and their satellite absorption lines. The present paper and paper II[13] deal only with one of these exciton lines, $A0$, and its satellite absorption lines, $A1$, $A2$, $H1$, $H2$, $H3$, and $H4$. The assignments of the $A1$, $A2$, and $H1$ lines are determined in paper II.[13]

The $H3$ line is assigned to the electronic transition from the thermally excited domain-wall state to the corresponding excited state of the $A0$ line. The $H4$ and $H2$ lines are concluded to be associated with the thermally excited singlet state, which is the second lowest excited state. The $H4$ line is attributed to the electronic transition from this singlet state to the corresponding excited state of the $A0$ line, and the $H2$ line is attributed to the $A0$ exciton creation at a site that is adjacent to such a singlet-state site along a chain.

Above about T_N (12.75 K), a single domain-wall excitation plays a very important role in the behavior of the spectra, and above about 20 K, domain-wall pair excitation also becomes important. Additionally, above about 30 K, excitation to the second lowest excited state is concerned with this behavior. Below T_N, the three-dimensional magnetic order suppresses the domain-wall movement.

The temperature variation of the intensities of the $A0$ and $H3$ lines conforms well to formulas (4) and (5), respectively, which are deduced from Boltzmann statistics taking account of the above-mentioned thermal excitations. This conformation shows that each of the domain walls is localized and stays within two adjacent sites during one excitation creation.

No hot-magnon sideband is observed below 77 K, because a magnon excited state transforms itself into two domain walls.

ACKNOWLEDGMENTS

The authors are deeply indebted to Dr. T. Kato of Kyoto University for the use of the Cary 17D grating spectrometer. H. O. gratefully acknowledges helpful discussions with Dr. I. Mogi of Tohoku University.

[1] J. A. J. Basten, Q. A. G. van Vlimmeren, and W. J. M. de Jonge, Phys. Rev. B **18**, 2179 (1978).

[2] H. Th. Le Fever, R. C. Thiel, W. J. Huiskamp, and W. J. M. de Jonge, Physica (Utrecht) **111B**, 190 (1981); H. Th. Le Fever, R. C. Thiel, W. J. Huiskamp, W. J. M. de Jonge, and A. M. van der Kraan, *ibid.* **111B**, 209 (1981).

[3] R. C. Thiel, H. de Graaf, and L. J. de Jongh, Phys. Rev. Lett. **47**, 1415 (1981).

[4] A. M. C. Tinus, C. J. M. Denissen, H. Nishihara, and W. J. M. de Jonge, J. Phys. C **15**, L791 (1982).

[5] J. P. M. Smeets, K. M. H. Maessen, E. Frikkee, and K. Kopinga, J. Magn. Magn. Mater. **31-34**, 1163 (1983).

[6] K. Kopinga, M. Steiner, and W. J. M. de Jonge, J. Phys. C **18**, 3511 (1985).

[7]J. P. M. Smeets, E. Frikee, W. J. M. de Jonge, and A. Kopinga, Phys. Rev. B **31**, 7323 (1985).

[8]M. Takeda, G. Kido, I. Mogi, Y. Nakagawa, H. Okada, and N. Kojima, J. Phys. Soc. Jpn. **58**, 3418 (1989).

[9]K. Kopinga, Q. A. G. van Vlimmeren, A. L. M. Bongaarts, and W. J. M. de Jonge, Physica (Utrecht) **86-88B**, 671 (1977).

[10]J. Villian, Physica (Utrecht) **79B**, 1 (1975).

[11]N. Ishimura and H. Shiba, Prog. Theor. Phys. **63**, 743 (1980).

[12]For a review, see. e.g., A. R. Bishop, J. A. Krumhansl, and S. E. Trullinger, Physica (Utrecht) **1D**, 1 (1980).

[13]H. Okada, N. Kojima, T. Ban, and I. Tsujikawa, following paper, Phys. Rev. B **42**, 11 619 (1990).

[14]The absorption line observed at about 24 320 cm^{-1} belongs to the A group and is assigned to the cooperative excitation of the $A0$ exciton and the electronic transition from the ground state to the third lowest excited state. This work does not deal with this absorption line.

[15]R. E. Deitz, A. Misetich, and H. J. Guggenheim, Phys. Rev. Lett. **16**, 841 (1966).

[16]R. Moncorge, B. Jacquier, and L. C. Brunel, J. Phys. Chem. Solids **43**, 155 (1982).

[17]I. Mogi, T. Okamoto, N. Kojima, T. Ban, and I. Tsujikawa, J. Phys. Soc. Jpn. **55**, 987 (1986).

[18]I. Mogi, N. Kojima, Y. Ajiro, H. Kikuchi, T. Ban, and I. Tsujikawa, J. Phys. Soc. Jpn. **56**, 4592 (1987); I. Mogi, M. Takeda, G. Kido, Y. Nakagawa, H. Kikuchi, and Y. Ajiro, *ibid.* **58**, 2188 (1989).

[19]Q. A. G. van Vlimmeren, C. H. W. Swüste, W. J. M. de Jonge, N. J. H. van der Steeg, J. H. M. Stoelinga, and P. Wyder, Phys. Rev. B **21**, 3005 (1980).